Power and Energy Characteristics of Solid-State Induced-Strain Actuators for Static and Dynamic Applications

VICTOR GIURGIUTIU* AND CRAIG A. ROGERS
Mechanical Engineering Department, University of South Carolina, Columbia, SC 29208

ABSTRACT: The power and energy characteristics of solid-state induced-strain actuators are studied. Piezoelectric (PZT), electrostrictive (PMN) and magnetostrictive (TERFENOL) actuators are considered. The principles and internal construction of solid-state induced-strain actuators are briefly reviewed. Typical performance curves are presented and discussed. The basic equations of piezoelectricity and piezomagnetism are presented. A linearization procedure is adopted whereby apparent values for the piezoelectric and piezomagnetic constants are derived from full-stroke vendor data using the secant approximation principle. Values for the apparent electromagnetic conversion coefficient for full-stroke operation are obtained.

The static analysis considers the one-directional operation of the induced strain actuators against an external spring load. It is found that the maximum energy output from the induced-strain actuator is obtained when the internal and external stiffnesses are matched. Expressions for the maximum energy output, and the energy densities per unit volume, mass, and cost are derived. Numerical examples and comparative charts are given for a number of piezoelectric, electrostrictive and magnetostrictive actuators. The influence of casing and pre-stress mechanism on the overall energy density values is also highlighted. The electromechanical conversion efficiency is studied, and two separate expressions are derived, one for the best efficiency, and another for the conversion efficiency at the stiffness match point.

The dynamic analysis considers the cyclic motion of the induced-strain actuators about a midpoint bias position. The dynamic full-stroke is found approximately one-half the static full-stroke. The correspondingly maximum output energy and energy densities under dynamic conditions are calculated. The dynamic energy conversion efficiency is studied and the influence of bias voltage or current is included. Numerical examples and comparative charts are given for a number of piezoelectric, electrostrictive and magnetostrictive actuators operating under dynamic conditions.

INTRODUCTION

THE use of solid-state induced-strain actuators has seen a great expansion in recent years. Initially developed for high frequency low-displacement acoustic applications, these revolutionary concepts are currently expanding their field of application into many other areas of mechanical and aerospace design. Compact and reliable, solid-state induced-strain actuators directly transform the input electrical energy into output mechanical energy. One application area in which solid-state induced-strain devices have a very promising perspective is that of linear actuation. Now, the linear actuation market is dominated by hydraulic and pneumatic cylinders and by electromagnetic solenoids and shakers. Hydraulic and pneumatic cylinders offer reliable performance, with high force and large displacement capabilities. When equipped with servovalves, the hydraulic cylinders can deliver variable stroke output over a relatively large frequency range. Servovalve-controlled hydraulic devices are the actuators of choice for most aerospace, automotive, and robotic applications. However, a major drawback in the use of conventional hydraulic actuators is the need for a separate hydraulic power unit equipped with large electric motors and hydraulic pumps that send the high-pressure hydraulic fluid to the actuators through hydraulic lines. These features can be a major drawback in certain applications. For example, in the actuation of a servo-tab placed at the tip of a rotating blade, the high-g environment, and the fact that the blade rotates, prohibit the use of conventional hydraulics. In such situations, and electromechanical actuation that directly converts electrical energy into mechanical energy is preferred.

Conventional electromechanical actuators, based on electric motors, either deliver rotary motion only, or use gearboxes and eccentric mechanisms to achieve linear motion. This route is cumbersome and leads to additional weight being added to that of the device, thus reducing its design effectiveness. Linear-action electromechanical devices, such as solenoids and electrodynamic shakers can be considered as alternatives, but are known for their typical low-force performance. The use of solenoids or electrodynamic shakers to perform the duty-cycle of hydraulic actuator is not presently conceivable. To these difficulties, solid-state induced-strain actuators offer a viable alternative. Though their output dis-

This article was presented at the *7th International Conference on Adaptive Structures Technology*, September 23–25, 1996, Rome, Italy.

*Author to whom correspondence should be addressed.

1045-389X/97/09 0738-13 $10.00/0
© 1998 Technomic Publishing Co., Inc.

placement is relatively small, they can produce remarkably high force. Through the use of well-architectured displacement amplification, induced-strain actuators can achieve dynamic output strokes similar to those of conventional hydraulic actuators. Additionally, unlike conventional hydraulic actuators, solid-state induced-strain actuators do not require separate hydraulic power units and long hydraulic lines, since they use the efficient route of electric supply.

The development of solid-state induced-strain actuators has entered the production stage, and actuation devices based on these concepts are likely to reach the applications market in the next few years. An increasing number of vendors are producing and marketing solid-state actuation devices based on induced-strain principles. However, the performance of the basic induced-strain actuation materials used in these devices, and the design solutions used in their construction, are found to vary from vendor to vendor. This variability presents a difficulty for the application engineer who simply wants to utilize the solid-state induced-strain actuators as prime movers in their design, and does not intend to detail the intricacies of active materials technology. Recognizing this need, the present paper sets out to perform a comparison of commercially available induced-strain actuators based on a common criterion: the amount of energy that they can deliver, and the energy density per unit volume, unit mass, and unit cost. Additionally, this paper also compares the efficiency with which various induced-strain actuators convert the input electrical energy into output mechanical energy. The comparison is done using vendor-supplied information collected in an extensive survey performed over several years. Both static and dynamic operational regimes are analyzed.

BASIC ASPECTS OF INDUCED-STRAIN ACTUATORS

Electroactive and Magnetoactive Materials

Active materials exhibit induced-strain actuation (ISA)** under the action of an electric or magnetic field. They are primarily of three types:

(a) PZT—Lead Zirconate Titanate—is a ferroelectric ceramic material with piezoelectric properties and reciprocal behavior that converts electrical energy into mechanical energy and vice-versa. A variety of PZT formulations have been developed to suit a wide range of signal transmission and reception qualities. PZT-5 is one of the most widely used formulations for actuator applications. The behavior of the PZT material is quasi-linear, though hysteretic. Reversed polarity can be accommodated in moderate quantities (25–30%).

(b) PMN—Lead Magnesium Niobate—An electrostrictive ceramic material with piezoelectric properties and reciprocal behavior that converts electrical energy into mechanical energy and vice-versa. PMN materials do not accept reverse polarity. Numerous PMN formulations have been developed to suit a wide range of signal transmission and reception qualities.

(c) TERFENOL—*TER* (Terbium) *FE* (Iron) *NOL* (Naval Ordinance Laboratory)—A magnetostrictive alloy consisting primarily of Terbium, Dysprosium, and Iron. In practice, TERFENOL materials are made to exhibit quasi-linear piezomagnetic behavior through the application of bias fields. Various TERFENOL formulations have been developed. A commonly used formulation is TERFENOL-D.

Construction of a PZT or PMN Stack Actuator

An electroactive solid-state actuator consists of a stack of many layers of electroactive material (PZT or PMN) alternatively connected to the positive and negative terminals of a high voltage source (Figure 1). Such a PZT or PMN stack behaves like an electrical capacitor. When activated, the electroactive material expands and produces output displacement. Typical strains for electroactive materials are in the range 0.075–0.150%. The PZT or PMN stacks are constructed by two methods. In the first method, the layers of active material and the electrodes are mechanically assembled and glued together using a structural adhesive. The adhesive modulus (typically 4–5 GPa) is at least an order of magnitude lower than the modulus of the ceramic (typically 70–90 GPa). This aspect may lead to loss in stack stiffness. In the second method, the ceramic layers and the electrodes are assembled in the "green" state, and then fired together (co-fired) in the processing oven. Compaction under high isostatic pressure (HIP process) is applied to improve mechanical behavior. This process ensures a much stiffer final product and, hence, better actuator performance. However, the processing limitations, such as oven and press sizes, etc., limit the process applicability to large stacks.

A polymeric or elastomeric protective wrapping surrounds the PZT and PMN stacks, with electrical connection wires protruding from the wrapping. Steel washers are used at the end of the stack to distribute the load into the brittle ce-

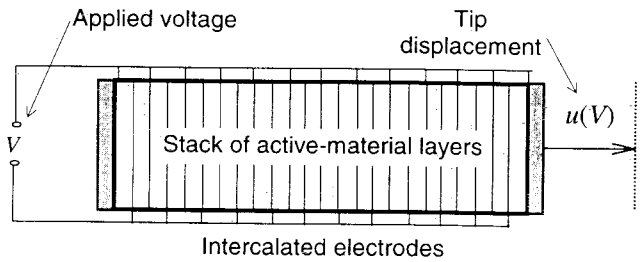

Figure 1. *Electroactive induced-strain actuator consisting of a stack of PZT or PMN wafers and intercalated electrodes.*

**The acronym ISA is used to signify either an induced-strain actuator, or the induced-strain actuation principle.

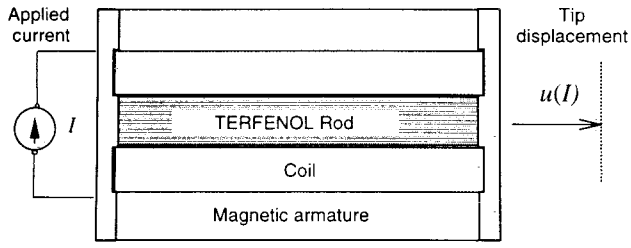

Figure 2. *Induced-strain actuator using a TERFENOL magnetoactive rod.*

ramic. Since ceramics and the connecting adhesive are weak in tension, care must be taken in practical applications to ensure that only compression load is applied to the stack. If tension loading also needs to be accommodated, adequate pre-stressing must be provided through springs or other means.

Construction of a TERFENOL Actuator

A magnetoactive solid-state actuator consists of a TERFENOL bar inside an electric coil enclosed into an annular magnetic armature (Figure 2). When the coil is activated, the TERFENOL expands and produces output displacement. The TERFENOL material has been shown to be capable of strains up to 2000 μm/m, but with highly nonlinear and hysteretic behavior. To keep the behavior in quasi-linear range, manufacturers of TERFENOL actuators limit their working strains to 1000 μm/m. The TERFENOL-D bar, the coil, and the magnetic armature are assembled between two steel washers and put inside a protective wrapping to form the basic magnetoactive induced-strain actuator.

Casing and Pre-Stress Mechanism

Some commercially available solid-state actuators also include a metal casing and a pre-stress mechanism. The casing provides protection for the active material and its electrical connections. It also facilitates the mechanical connection of the induced-strain actuator to the application structure. The pre-stress mechanism ensures that the active material sees only compression, even with moderate tension applied to the output rod. When a pre-stress mechanism is incorporated, the protective casing must act as the return path for the spring load. The actuators with casing and pre-stress mechanism are easier to incorporate into the application structure, but are heavier than mere stacks.

Typical Performance of Solid-State Induced-Strain Actuators

Figures 3 through 5 illustrate typical performance of commercially available solid-state induced-strain actuators under no-load condition. Figure 3 presents the voltage-displacement relationship for the PZT actuator P-245-70 produced by Polytec PI, Inc. (1995) measured by the authors during a laboratory test (Giurgiutiu and Rogers, 1997a). It is noted that the stack can produce a maximum expansion of value $u_{ISA}^{+} = 120$ μm. Piezoelectric stacks also accept reverse polarity up to 25–30%. The corresponding maximum contraction is $u_{ISA}^{-} = -30$ μm. (For stack-safety reasons, our experiments were not conducted to the maximum contraction level.) The total static travel of this actuator is $u_{ISA}^{static} = 150$ μm. Since the stack length was $l = 100$ mm, the static free strain of this stack is $\varepsilon_{ISA}^{static} = 0.150\%$. For dynamic applications, the actuator is electrically biased about a mid-range position and then an alternating voltage is superimposed. For the present example, the bias position would be $u_0 = (1/2)(u_{ISA}^{+} + u_{ISA}^{-}) = 45$ μm, while the alternating component would be, $u_{ISA}^{dynamic} = \pm 75$ μm. The dynamic free-strain is $\varepsilon_{ISA}^{dynamic} = \pm 75\%$. Figure 3 also shows that this induced-strain actuator has significant hysteresis, which is typical of PZT stacks.

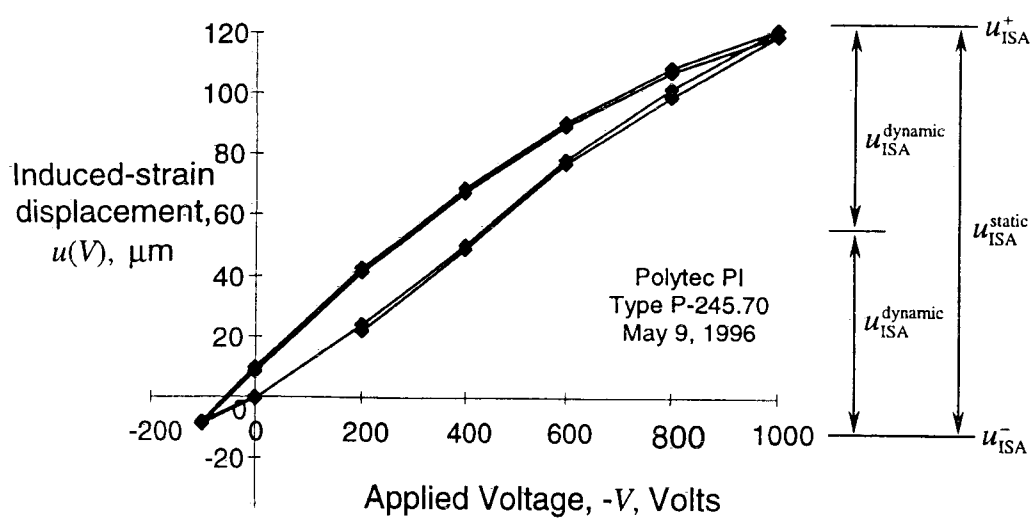

Figure 3. *Induced-strain displacement vs. applied voltage for Polytec PI model P-245.70 piezoelectric (PZT) actuator.*

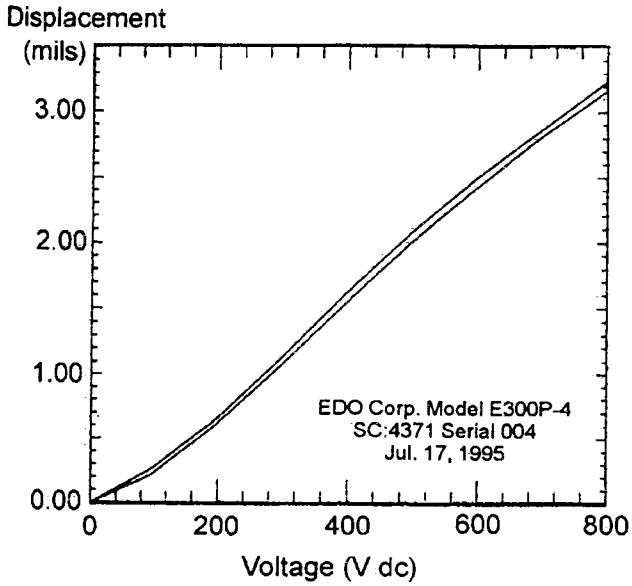

Figure 4. *Induced-strain displacement vs. applied voltage for EDO Corp. model E300P-4 electrostrictive (PMN) actuator.*

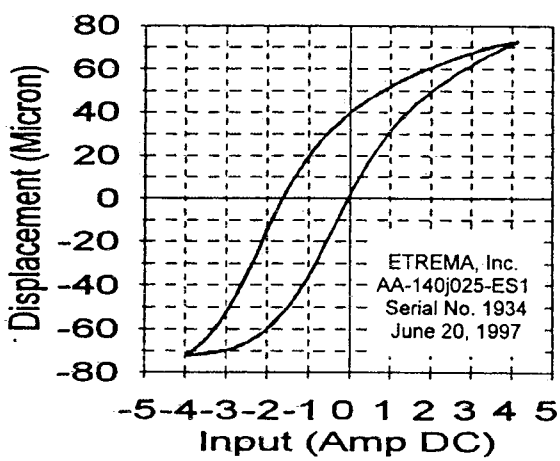

Figure 5. *Induced-strain displacement vs. applied voltage for ETREMA, Inc. model AA-140J025-ES1 magnetostrictive (TERFENOL-D) actuator.*

Figure 4 presents the voltage-displacement curve for the PMN actuator E300P-4 produced by EDO Corporation (1996), as measured by the manufacturer. The maximum expansion is $u_{ISA}^{+} = 3.2$ mil = 81 μm. PMN materials do not accept reversed polarity, hence $u_{ISA}^{-} = 0$. Thus the total free stroke of this induced-strain actuator is merely $u_{ISA}^{static} = 81$ μm. Since the stack length was $l = 2.4$ in = 61 mm, the corresponding free strain of this stack is $\varepsilon_{ISA}^{static} = 0.133\%$. If the actuator were to be used for dynamic applications, the dynamic free stroke would be $u_{ISA}^{dynamic} = \pm 40$ μm, with the corresponding dynamic free strain $\varepsilon_{ISA}^{dynamic} = \pm 0.67\%$. Figure 4 also shows that this induced-strain actuator has very little hysteresis, typical of PMN stacks.

Figure 5 presents the current-displacement curve for the TERFENOL actuator AA140J013-ES1 produced by ETREMA, Inc. (1997), as measured by the manufacturer. This actuator was specially biased for dynamic operation. Thus, the maximum expansion and the maximum contraction have equal magnitudes, i.e., $u_{ISA}^{+} = u_{ISA}^{-} = u_{ISA}^{dynamic} = 70$ μm. The total free stroke of this induced-strain actuator is $u_{ISA}^{static} = 140$ μm. Since the length of the TERFENOL rod was $l = 140$ mm, the corresponding free strain of this induced strain actuator is $\varepsilon_{ISA}^{static} = 0.100\%$. For dynamic operation, the dynamic free strain is $\varepsilon_{ISA}^{dynamic} = \pm 0.50\%$. Figure 5 also shows that this induced-strain actuator has significant hysteresis.

THEORETICAL BACKGROUND

Basic Equations of Piezoelectricity and Piezomagnetism

The general constitutive equations of linear piezoelectricity, given by ANSI/IEEE Standard 176-1987 (Anon., 1988) describe a tensorial relation between mechanical and electrical variables (mechanical strain S_{ij}, mechanical stress T_{ij}, electrical field E_i, and electrical displacement D_i in the form:

$$\begin{aligned} S_{ij} &= s_{ijkl}^{E} T_{kl} + d_{kij} E_k \\ D_j &= d_{jkl} T_{kl} + \varepsilon_{jk}^{T} E_k \end{aligned} \tag{1}$$

where s_{ijkl}^{E} is the mechanical compliance of the material measured at zero electric field ($E = 0$), ε_{jk}^{T} is the dielectric permittivity measured at zero mechanical stress ($T = 0$), and d_{kij} is the piezoelectric coupling between the electrical and mechanical variables.

Typical electroactive induced-strain actuators are stacks of thin active-material layers, alternatingly charged (Figure 1). In such an electroactive material stack, mechanical stress and electric field act only in the 3-direction (the stack axis), and the transverse effects can be neglected in a first-order analysis. The one-dimensional equivalent of Equations (1) is

$$S = s \cdot T + d \cdot E$$
$$D = d \cdot T + \varepsilon \cdot E \tag{2}$$

where the subscripts "3," "33," "333," and "3333" are implied, as appropriate, while s is the compliance measured at zero electric field, and ε is the permittivity measured at zero stress.

For magnetoactive materials, a set of equations similar to Equations (1) can also be derived:

$$S_{ij} = s^E_{ijkl} T_{kl} + d_{kij} H_k$$
$$D_j = d_{jkl} T_{kl} + \mu^T_{jk} H_k \tag{3}$$

where H_k is the magnetic field intensity, and μ^T_{jk} is the magnetic permeability under constant stress. The coefficients d_{kij} are now defined in terms of magnetic units. The magnetic field intensity H in a rod of length L is related to the current in the surrounding coil (with n turns per unit length) through the expression:

$$H = nI \tag{4}$$

Linearized Electromechanical Behavior of Solid-State Induced-Strain Actuators

As illustrated in Figures 3 through 5, the field-displacement behavior of induced-strain actuators is not perfectly linear. However, quasi-linear behavior can be assumed using the secant approximation of the full-stroke values. Apparent electromechanical and magnetomechanical constants for electroactive and magnetoactive induced-strain actuator result. Thus, the overall performance of the induced-strain actuators can be defined in terms of readily available vendor data, such as : free-stroke, u_{ISA}, the corresponding voltage, V (or current, I), the internal stiffness, k_i, and the capacitance, C (or inductance, L). This approach predicts the power and energy ratings of induced-strain actuators under full-stroke operation in a straightforward easy-to-understand manner.

Apparent values of the piezoelectric strain coefficient, d, elastic compliance, s, and electrical permittivity, ε, are given by:

$$d = \frac{u_{ISA}}{V}\frac{t}{l} \quad \text{(apparent piezoelectric strain coefficient)}$$

$$\varepsilon = \frac{C}{A}\frac{t^2}{l} \quad \text{(apparent zero-stress electrical permittivity)}$$

$$s = \frac{A}{lk_i} \quad \text{(apparent zero-field elastic compliance)}$$

(5a)–(5c)

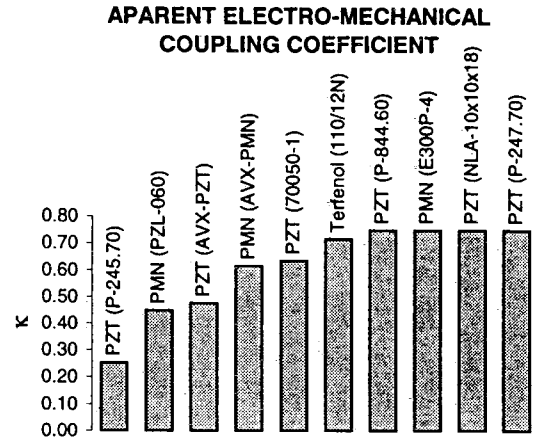

Figure 6. *Apparent electromechanical coupling coefficient, κ, for several solid-state induced-strain actuators (PZT, PMN, TERFENOL).*

where l is the stack length, t is the layer thickness, A is the stack cross-sectional area, and u_{ISA} is the dynamic free stroke. According to the IEEE Standard on piezoelectricity (ANSI/IEEE Std 176-1987), the electromechanical coupling coefficient, relevant to the 33-direction in which induced-strain actuators operates, is:

$$(k^l_{33})^2 = \frac{d^2_{33}}{s^E_{33}\varepsilon^T_{33}} \tag{6}$$

Consistent with the linearization scheme, the constants d_{33}, ε^T_{33}, and s^E_{33}, are given by expressions (5a)–(5c) as d, ε, and s. Denoting k^l_{33} by κ (to avoid confusion with the notation, k, already used for the mechanical stiffness) the following simple expression for the full-stroke electromechanical coupling coefficient of the actuator is obtained:

$$\kappa^2 = \frac{d^2}{s\varepsilon} = \frac{k_i u^2_{ISA}}{CV^2} \tag{7}$$

For piezomagnetic actuators, a similar process is employed with current, I, and inductance, L, replacing voltage, V, and capacitance, C, i.e.,

$$\kappa^2 = \frac{d^2}{s\mu} = \frac{k_i u^2_{ISA}}{LI^2} \tag{8}$$

Figure 6 presents numerical values of the apparent electromechanical coupling coefficient, κ, for a variety of induced-strain actuators (PZT, PMN, TERFENOL).

STATIC ANALYSIS

Many solid-state induced-strain actuators are used in static and quasi-static regime, e.g., micropositioning appli-

cations or on-off actuation. In this case, frequency effects are ignored and simple equations based on the static characteristics can be derived. Figure 7 shows a solid-state induced-strain actuator operating a spring-like mechanical load, k_e. When the actuator is energized, the active material expands and produces an output displacement, u, which generates a reaction force, F, from the mechanical system. Due to actuator compressibility, the force, F, produces an elastic internal displacement, F/k_i, where k_i is the internal stiffness. Since induced-strain actuators have finite internal stiffness, the application of an external load will always be accompanied by compressibility loss and the output displacement, u_e, will only be a fraction of its induced-strain displacement, u_{ISA}. Using the stiffness ratio, $r = k_e/k_i$, one writes:

$$u_e = \frac{1}{1+r} u_{ISA} \tag{9}$$

Defining the output energy as half the product between force and output displacement, one writes:

$$E_{out} = E_e = \frac{1}{2} F_e \cdot u_e = \frac{1}{2} k_e \cdot u_e^2 \tag{10}$$

where $F = k_e \cdot u_e$. Substitution of Equation (9) into Equation (10) yields the expression of output energy in terms of stiffness ratio, r, i.e.,

$$E_{out}(r) = \frac{r}{(1+r)^2}\left(\frac{1}{2} k_i u_{ISA}^2\right) = \frac{r}{(1+r)^2} E_{mech}^2 \tag{11}$$

The constant part of Equation (11) is the reference mechanical energy resulting from electromechanical conversion, $E_{mech}^* = (1/2)k_i u_{ISA}^2$. The variable part of Equation (11) is the output energy coefficient:

$$E'_{out} = \frac{r}{(1+r)^2} \tag{12}$$

representing the percentage of energy that can be extracted from the stack to perform useful external work. A plot of $E'_{out}(r)$ as a function of r is given in Figure 8. The function $E'_{out}(r)$ is zero for both "free" ($r = 0$) and "blocked" ($r \to \infty$) conditions, and has a maximum at $r = 1$ (stiffness match). Its maximum value is $(E'_{out})_{max} = 1/4$. Thus, the maximum output energy that can be extracted from an induced-strain actuator under the most favorable conditions is:

$$E_{out}^{max} = \frac{1}{4} E_{mech}^* = \frac{1}{4}\left(\frac{1}{2} k_i u_{ISA}^2\right) \tag{13}$$

Equation (13) shows that no more than 25% of the reference energy, $E_{mech}^* = (1/2)k_i u_{ISA}^2$, can be actually extracted from the actuator.

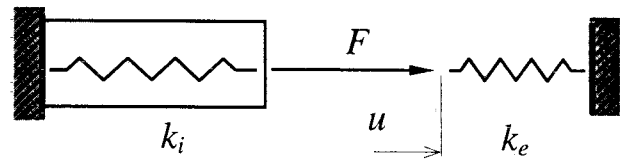

Figure 7. *Schematic representation of a solid-state induced-strain actuator (PZT stack) operating against a mechanical load under static conditions.*

Example: The Polytec PI actuator P247-70 produces a free displacement $u_{ISA} = 150$ μm, and has an internal stiffness $k_i = 370$ kN/mm. Under the most favorable conditions (i.e., at stiffness match), the output energy will be $E_{out}^{max} = (1/4)[(1/2)370\ \text{N/μm} \cdot (150\ \text{μm})^2] = 1.041$ J.

Output Energy Densities

In order to compare the output performance of induced-strain actuators of different shapes and sizes, allowance must be made for their differences in volume and mass. This study uses two output energy densities: the specific output energy per unit volume and the specific output energy per unit mass. They are computed by simply dividing the maximum output energy by the volume and the mass of the actuator, respectively. Output energy per unit cost is also studied.

Energy Conversion Efficiency

The output mechanical energy delivered by an induced-strain actuator results from electromechanical conversion of the applied electrical energy through the piezoelectric or piezomagnetic effects. For electroactive solid-state actuators (PZT and PMN) under no-load conditions, the electrical energy has the reference value:

$$E_{elec}^* = \frac{1}{2} C V^2 \tag{14}$$

When external load is applied through, say, an elastic spring, the effective capacitance is modulated by the stiffness ratio (Giurgiutiu, Chaudhry and Rogers, 1994):

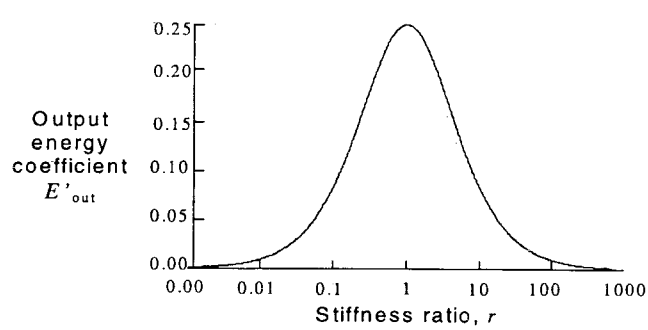

Figure 8. *Variation of output energy coefficient, E'_{out} with stiffness ratio, r, showing a peak equal to 1/4 at r = 1.*

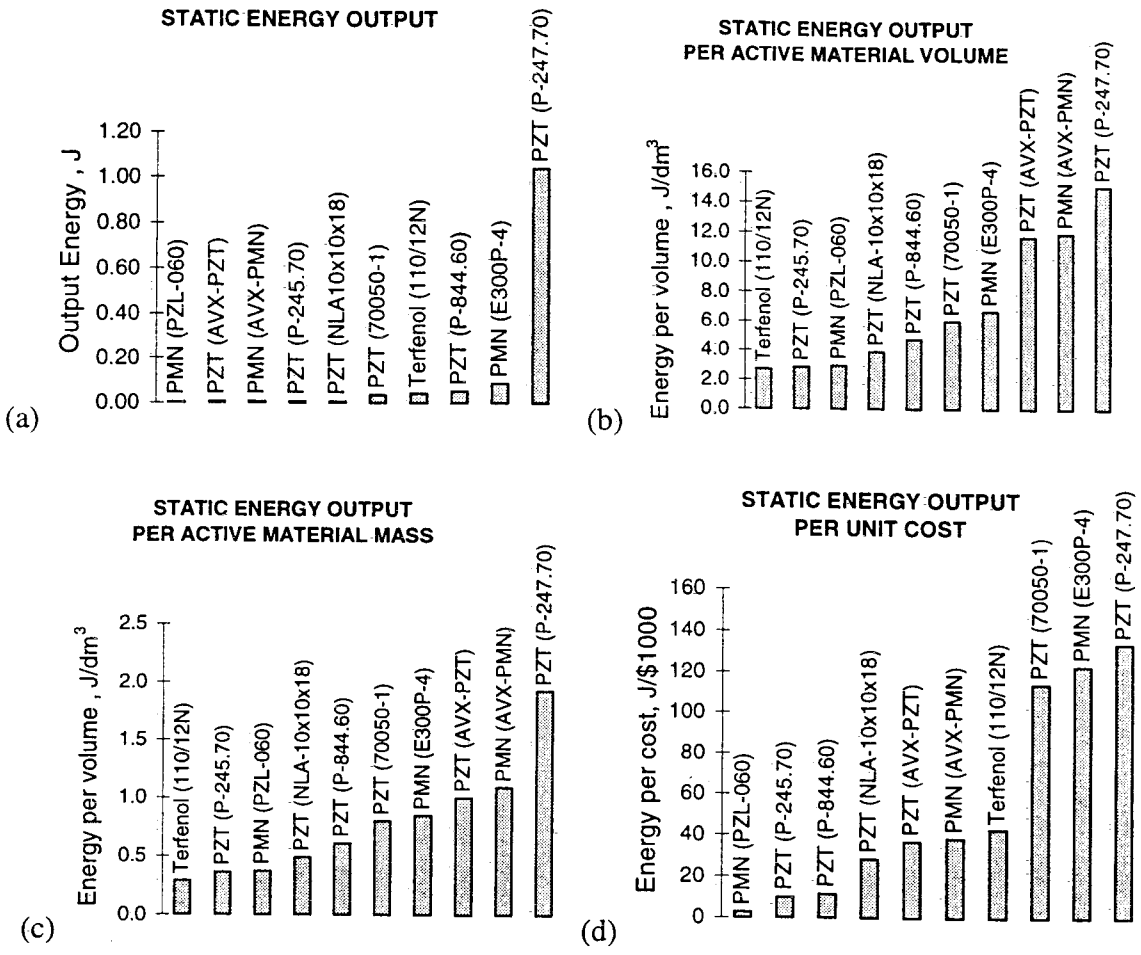

Figure 9. *Energy and energy density comparison of solid-state induced-strain actuators (PZT, PMN, TERFENOL) operating under static operation.*

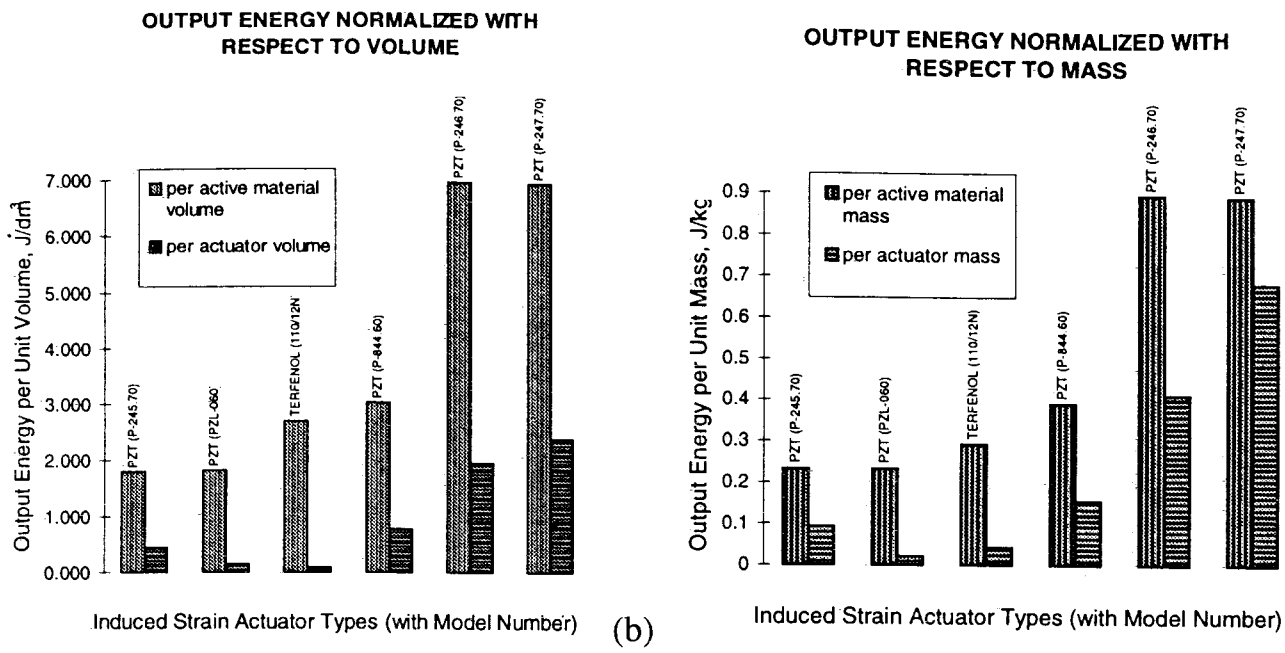

Figure 10. *The addition of casing greatly reduces the volume-based energy density due to the large relative volume of the casing: (a) energy density per unit volume; (b) energy density per unit mass.*

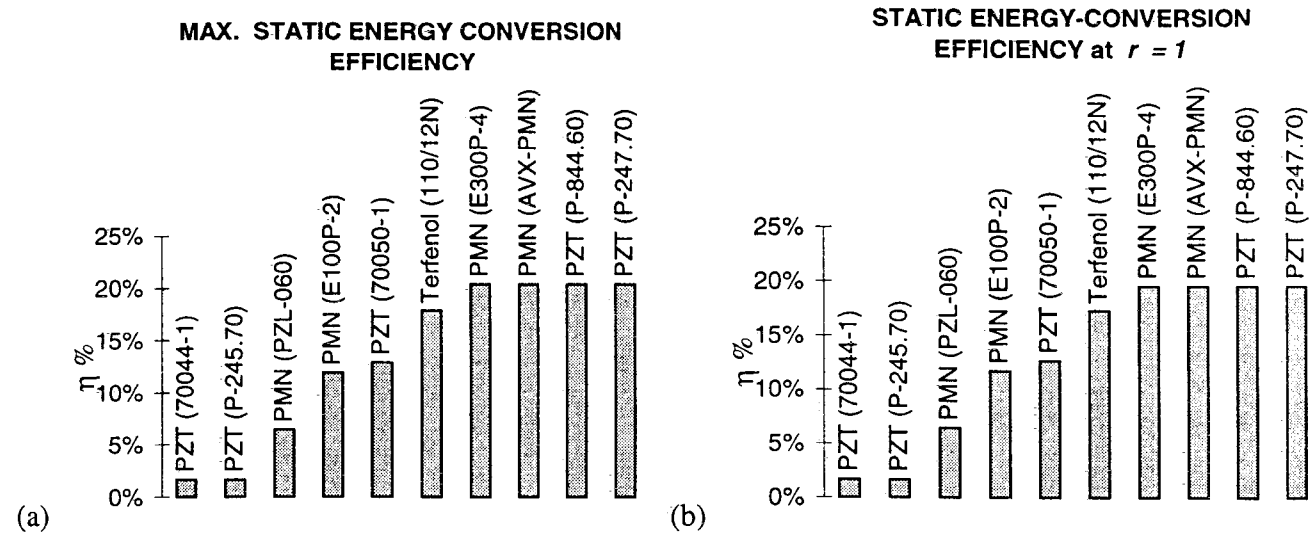

Figure 11. *Comparison of energy conversion efficiency of several solid-state induced-strain actuators (PZT, PMN, and TERFENOL) under static operation: (a) maximum energy conversion efficiency; (b) energy conversion efficiency at stiffness match (r = 1).*

$$Y(\omega) = i\omega C\left(1 - \kappa^2 \frac{\bar{r}(\omega)}{1 + \bar{r}(\omega)}\right) \tag{15}$$

and hence,

$$E_{elec}(r) = \left(1 - \kappa^2 \frac{r}{1+r}\right)\left(\frac{1}{2}CV^2\right) = \left(1 - \kappa^2 \frac{r}{1+r}\right)E^*_{elec} \tag{16}$$

Similarly, for magnetoactive solid-state actuators,

$$E_{elec}(r) = \left(1 - \kappa^2 \frac{r}{1+r}\right)\left(\frac{1}{2}LI^2\right) = \left(1 - \kappa^2 \frac{r}{1+r}\right)E^*_{elec} \tag{17}$$

The energy conversion coefficient is simply defined as the ratio between output mechanical energy and input electrical energy

$$\eta = E_{out}/E_{in} \tag{18}$$

Substituting Equations (7) and (16) into Equation (18) and recalling $\kappa^2 = E^*_{mech}/E^*_{elec}$ gives:

$$\eta = \frac{1}{4}\left(\frac{\kappa^2}{1 - \kappa^2 \dfrac{r}{r+1}}\right) \tag{19}$$

Equation (19) has a maximum at $r^* = 1/\sqrt{1-\kappa^2}$ with the value

$$\eta_{max} = \frac{\kappa^2}{2\sqrt{1-\kappa^2} + 2 - \kappa^2} \tag{20}$$

On the other hand, the conversion efficiency at the stiffness match point ($r = 1$) is

$$\eta_{r=1} = \frac{1}{2}\left(\frac{\kappa^2}{2 - \kappa^2}\right) \tag{21}$$

Note that the maximum energy conversion efficiency, η_{max}, and the conversion efficiency at the stiffness match point, $\eta_{r=1}$, are different. In application design, either of the two efficiencies can be optimized, but not both. In other words, one can either design for maximum energy output by imposing the stiffness match condition ($r = 1$), or can design for maximum conversion efficiency by choosing $r^* = 1/\sqrt{1-\kappa^2}$. However, for practical applications, the numerical difference between the two results is small.

Numerical Results for Static Operation

Figure 9 presents comparative static energy data for a variety of induced-strain actuators (PZT, PMN, and TERFENOL). The maximum static energy output and the static energy density per unit volume, mass and cost are presented. Figure 10 compares energy density of induced-strain actuators with and without casing. Figure 11 presents the energy conversion efficiency for static operation. Two cases are shown: (a) maximum conversion efficiency; (b) conversion efficiency at the stiffness match point. Note that, for the solid-state induced-strain actuators considered in this study, the two cases give similar numerical results.

DYNAMIC ANALYSIS

As illustrated in Figures 3 through 5, solid-state induced-strain actuators may or may not have symmetrical behavior with respect to polarity reversal. For example, PZT stacks accept some reverse polarity (Figure 3), PMN stacks do not accept any polarity reversal (Figure 4) while TERFENOL actuators can be internally biased to accept complete polarity reversal (Figure 5). In the most general case, dynamic operation of a solid-state actuator can be assumed to take place about a mid-range position by superposing dynamic voltage amplitude onto a bias voltage component:

$$v(t) = V_0 + V \sin \omega t \tag{22}$$

where V_0 is the bias voltage, and V is the dynamic voltage amplitude. The corresponding induced-strain displacement will be:

$$u(t) = u_0 + \hat{u}_{ISA} \sin \omega t \tag{23}$$

where u_0 is the bias position, and $\hat{u}_{ISA}$ is the dynamic displacement (Figure 12).

Induced-Strain Actuator Operating a Dynamic Load

Figure 13 shows a solid-state induced-strain actuator operating against a dynamic load of parameters $k_e(\omega)$, $m_e(\omega)$, and $c_e(\omega)$. The actuator is energized by a variable voltage, $v(t)$, which sends a current, $i(t)$. Under the energizing action, the active material expands and produces an output displacement, $u(t)$, which generates a dynamic reaction force, $F(t)$. The reaction force, $F(t)$, acting on the induced-strain actuator, induces loss of output displacement through internal compressibility and through the counter electric motive force (back emf) due to the piezoelectric or piezomagnetic effect. For relatively low operation frequencies, the wave propagation effects can be ignored, and the equivalent input admittance is given by (Giurgiutiu, Chaudhry, and Rogers, 1994):

$$Y(\omega) = i\omega C\left(1 - \kappa^2 \frac{\bar{r}(\omega)}{1 + \bar{r}(\omega)}\right) \tag{24}$$

where $\kappa^2 = d^2/(\bar{s} \cdot \bar{\varepsilon})$ and

$$\bar{s} = (1 - i\delta_s)s, \quad \bar{\varepsilon} = (1 - i\delta_\varepsilon)\varepsilon \tag{25}$$

with δ_s being the hysteresis internal damping coefficient, and δ_ε the dielectric loss coefficient. The coefficient $\bar{r}(\omega)$ is the complex stiffness ratio:

$$\bar{r}(\omega) = \bar{k}_e(\omega)/\bar{k}_i \tag{26}$$

where the complex stiffness expressions are:

$$\bar{k}_i = \frac{A}{\bar{s}\, l} \qquad \text{(complex internal stiffness)}$$

$$\bar{k}_e(\omega) = (k_e - \omega^2 m_e) + i\omega c$$

(complex external stiffness)

(27a)–(27b)

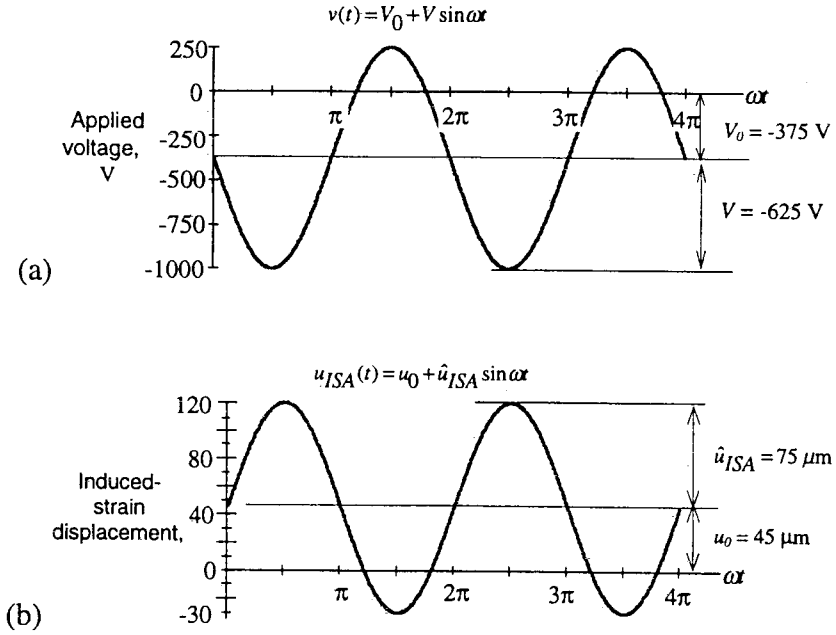

Figure 12. Dynamic operation of Polytec PI P247.70 induced-strain actuator: (a) applied voltage, v(t), has bias and dynamic components, V_0 and V; (b) the corresponding induced-strain displacement, $u_{ISA}(t)$.

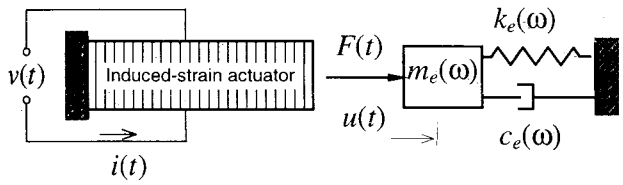

Figure 13. *Schematic representation of a solid-state induced-strain actuator (PZT stack) operating against a mechanical load under dynamic conditions.*

Similar expressions can be derived for magnetoactive materials, i.e.,

$$Z(\omega) = i\omega L\left(1 - \kappa^2 \frac{\bar{r}(\omega)}{1+\bar{r}(\omega)}\right) \tag{28}$$

Mechanical Power Output from an Induced-Strain Actuator

By definition, *mechanical power = force × velocity*. For harmonic motion, the expression of the complex power is $\bar{P} = (1/2)\bar{F} \cdot \bar{v}^*$, where, $\bar{v}^*$ is the complex conjugate of $\bar{v}$, and $\bar{v} = i\omega\bar{u}$. Using the output displacement amplitude

$$\bar{u} = \frac{1}{1+\bar{r}(\omega)}\hat{u}_{ISA} \tag{29}$$

we write the output mechanical power as:

$$\bar{P}_{mech} = \frac{1}{2}\bar{k}_e\bar{u}(i\omega\bar{u})^*$$

$$= -i\omega\frac{\bar{r}(\omega)}{(1+\bar{r}(\omega))(1+\bar{r}(\omega))^*}\left[\frac{1}{2}k_i\hat{u}_{ISA}^2\right] \tag{30}$$

Equation (30) is the dynamic equivalent of Equation (11) derived for static operation. If the mechanical load is lightly damped, and if the system operates well below the mechanical resonance frequency, the complex stiffness ratio can be approximated by its real part, i.e., $\bar{r}(\omega) \approx r$. Hence, the output power amplitude is

$$P_{out} = |\bar{P}_{mech}| = \omega\frac{r}{(1+r)^2}E_{mech}^* \tag{31}$$

where $E_{mech}^* = (1/2)k_i\hat{u}_{ISA}^2$. However, the dynamic E_{mech}^* is different from the static E_{mech}^* since the static value u_{ISA} is different from the dynamic value $\hat{u}_{ISA}$. The power can also be expressed as $P_{out} = \omega \cdot E_{out}$, where

$$E_{out} = \frac{r}{(1+r)^2}E_{mech}^* \tag{32}$$

Since ω may vary from application to application, the power values may also vary. However, this does not happen with the dynamic energy given by Equation (32). Hence, Equation (32) gives a consistent metric for comparing induced-strain actuators under dynamic operation in the dynamic energy output. Equation (32) is similar to Equation (11) from static analysis. However, the dynamic E_{mech}^* is different from the static E_{mech}^* since the static value u_{ISA} is different from the dynamic value $\hat{u}_{ISA}$. At the stiffness match point ($r = 1$),

$$P_{out}^{max} = \omega\frac{1}{4}E_{mech}^* \tag{33}$$

Electrical Power Input to an Induced-Strain Actuator

By definition, *electrical power = voltage × current*, and hence,

$$P(t) = v(t)\cdot i(t) = (V_0 + V\sin\omega t)\cdot I\sin(\omega t - \phi) \tag{34}$$

Expansion of Equation (34) gives:

$$P(t) = P_{active} + P_{reactive}(t) \tag{35}$$

where $P_{active} = (1/2)VI\cos\phi$ and $P_{reactive}(t) = (1/2)VI(-\cos(2\omega t - \phi) + 2v_0\sin(\omega t - \phi))$. The amplitude of the reactive power is the complex power amplitude, $|\bar{P}| = (1/2)VI$. Solid-state induced-strain actuators are either dominantly capacitive (PZT or PMN), or dominantly inductive (TERFENOL). Hence, the active power factor $\cos\phi$ is small and only becomes a concern at high frequencies when it can result in excessive internal heating. The dominant reactive power represents the main concern in applications since it dictates the rating of the power supply. As shown by Giurgiutiu and Rogers (1997b), the peak reactive power under bias operation ($v(t) = V_0 + V\sin\omega t$) can be approximated by:

$$P_{reactive}^{peak} = \chi(v_0)|\bar{P}| \tag{36}$$

where $v_0 = V_0/V$ or I/I_0, and $\chi(v_0) \approx 1 + 1.62|v_0|$. For electroactive induced-strain actuators, $|\bar{P}| = (1/2)|Y \cdot V^2|$, where the admittance $Y(\omega) = i\omega C\{(1-\kappa^2)[\bar{r}(\omega)]/[1+\bar{r}(\omega)]\}$ is frequency dependent. For magnetoactive induced-strain actuators, $|\bar{P}| = (1/2)|Z \cdot I^2|$, with $Z(\omega) = i\omega L\{(1-\kappa^2)[\bar{r}(\omega)]/[1+\bar{r}(\omega)]\}$. Defining the input electrical power as the peak reactive power yields:

$$P_{elec} = \omega\cdot\chi(v_0)\left|1 - \kappa^2\frac{\bar{r}(\omega)}{1+\bar{r}(\omega)}\right|\cdot E_{elec}^* \tag{37}$$

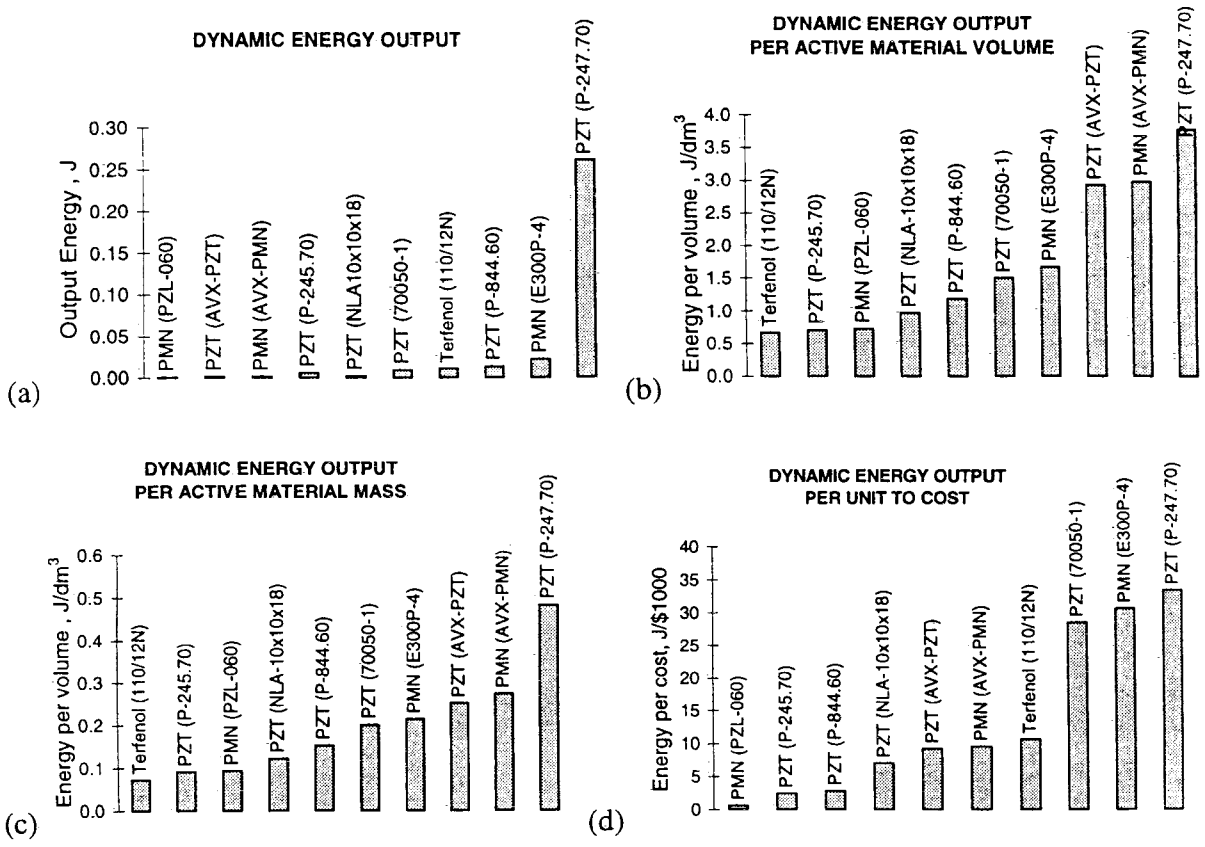

Figure 14. *Energy and energy density comparison of solid-state induced-strain actuators (PZT, PMN, TERFENOL) operating under dynamic operation.*

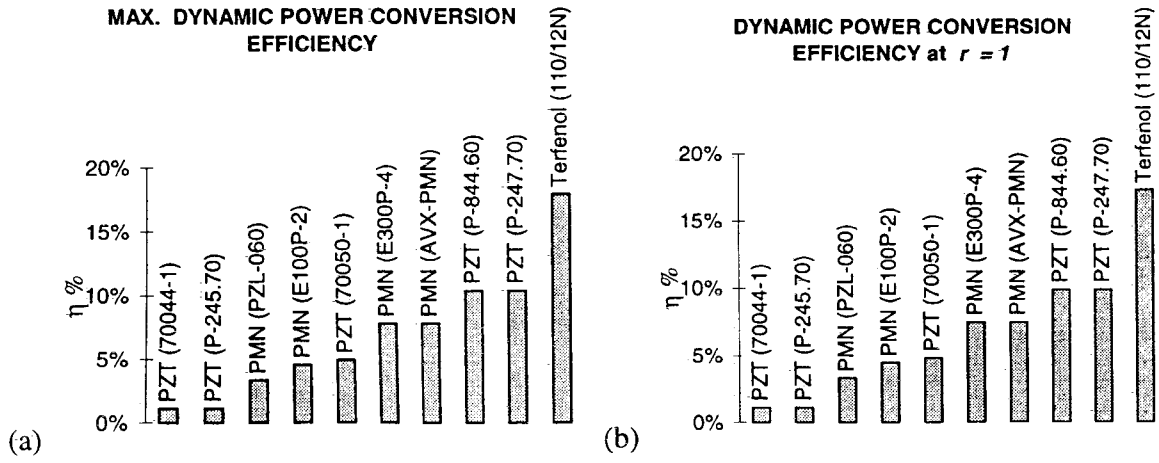

Figure 15. *Comparison of energy conversion efficiency of several solid-state induced-strain actuators (PZT, PMN, and TERFENOL) under dynamic operation: (a) maximum energy conversion efficiency; (b) energy conversion efficiency at stiffness match (r = 1).*

where the reference electrical energy is $E^*_{elec} = (1/2)C \cdot V^2$ or $E^*_{elec} = (1/2)L \cdot I^2$, as appropriate. Equation (37) is the dynamic equivalent of Equation (16) derived for static operation. Note that though apparently the same, E^*_{elec} has different values under dynamic operation than under static operation since the static and dynamic values of V or I are substantially different. If the mechanical load is lightly damped, and if the system operates well below the mechanical resonance frequency, the complex stiffness ratio can be approximated by its real part, i.e., $\bar{r}(\omega) \approx r$. Thus, the expression of input power is

$$P_{in} = \omega \cdot E_{in} \tag{38}$$

where E_{in} the peak input energy per cycle under dynamic operation. For stiffness match ($r = 1$),

$$E_{in} = \chi(v_0)\left(1 - \frac{1}{2}\kappa^2\right) \cdot E^*_{elec} \tag{39}$$

Power Conversion Efficiency

The power conversion efficiency is simply defined as the ratio between output mechanical power and input electrical power, i.e.,

$$\eta = \frac{P_{out}}{P_{in}} \tag{40}$$

Using Equations (33) and (38), and recalling that $\kappa^2 = E^*_{mech}/E^*_{elec}$ yields the overall power conversion efficiency:

$$\eta = \frac{1}{4}\left(\frac{\kappa^2}{1 - \kappa^2 \dfrac{1}{r+1}}\right)\Big/\chi(v_0) \tag{41}$$

As in the static case, two important cases need to be considered:

(a) the maximum conversion efficiency

$$\eta = \frac{\kappa^2}{2\sqrt{1-\kappa^2} + 2 - \kappa^2}\Big/\chi(v_0) \tag{42}$$

(b) the conversion efficiency at the stiffness match point ($r = 1$)

$$\eta = \frac{1}{2}\left(\frac{\kappa^2}{2 - \kappa^2}\right)\Big/\chi(v_0) \tag{43}$$

Expressions (42) and (43) are similar to the expressions (20) and (21) derived for the static case, only that a new term, $\chi(v_0)$, due to the bias voltage or current, has been included.

Numerical Results for Dynamic Operation

Figure 14 presents the output energy and energy densities for dynamic operation. The maximum dynamic energy per cycle and the dynamic energy densities per unit volume, mass, and cost are presented. To find the corresponding power, one needs to multiply the energy values by the angular frequency of operation. Figure 15 presents the maximum conversion efficiency, η_{max}, and the stiffness-match conversion efficiency, $\eta_{r=1}$, for dynamic operation.

CONCLUSIONS

The static and dynamic power and energy capabilities of commercially available solid-state induced-strain actuators have been considered. Piezoelectric (PZT), electrostrictive (PMN) and magnetostrictive solid-state actuators have been studied. The principles and internal construction of these devices had been briefly described. Typical performance curves, showing the relationship between output displacement and applied voltage or current have been presented. It was found that PZT and TERFENOL actuators present pronounced hysteresis, while PMN actuators have almost no hysteresis. However, PZT and TERFENOL actuators allow for polarity reversal (25% for PZT, 100% for magnetically biased TERFENOL) while PMN actuators do not.

The basic equations of piezoelectricity and piezomagnetism have been reviewed and applied to the study of solid-state induced-strain actuators. For full-stroke analysis, a secant approximation method was applied to obtain equivalent quasi-linear characteristics. Thus, the apparent electromechanical coupling coefficient κ, could be derived. This coefficient was found a very efficient instrument for the initial screening of the induced-strain actuators and validation of vendor data.

The static analysis was performed assuming the induced-strain actuator acting against a spring-like mechanical load. A static stiffness ratio was defined as the ratio between the external stiffness of the mechanical load and the internal stiffness of the actuator. Expressions for the output displacement and output energy as functions of the stiffness ratio were derived. The maximum energy output was found when matching exists between the external stiffness and the internal stiffness of the actuator ($r = 1$). The input electrical energy required to drive the actuator at various stiffness ratios was also calculated. Hence, the global electromechanical conversion efficiency of the actuator could be calculated. It was found that the maximum efficiency takes place at $r^* = 1/\sqrt{1-\kappa^2}$, which is different from the stiffness match value $r = 1$. Hence, design optimization of induced-strain actuators can be done either for maximum energy output ($r = 1$), or for maximum conversion efficiency ($r = r^*$). Numerical values for the output energy, output energy density per unit volume, mass, and cost were calculated and comparatively presented for a set of PZT, PMN and TERFENOL actuators. The influence of casing volume and mass on the overall energy density were also studied.

The dynamic analysis was performed for a mechanical load modeled by a spring-mass-damping system. The stiffness, mass and damping were allowed to vary with the excitation frequency. A dynamic stiffness ratio $\bar{r}(\omega)$ was defined as the ratio between the frequency-dependent complex stiffness of the external system and the complex internal stiffness of the actuator. It was found that for lightly damped systems, the reactive power and energy are dominant, which is fundamentally different from the conventional analysis of electric motors and other electromechanical devices. A reactive power amplification coefficient, $\chi(v_0)$, was defined in terms of the complex power magnitude, $|\bar{P}| = |\bar{Y}|V^2$, and the bias coefficient, v_0. Hence, the reactive input power requirements for an electroactive induced-strain actuator could be expressed in terms of the complex stiffness ratio, $\bar{r}(\omega)$ and the bias coefficient v_0. The dynamic output power and energy were calculated ($\hat{P}_{out}^{max} = \omega \hat{E}_{out}^{max}$). Since power depends linearly on frequency and energy, it was found that a better metric for actuator comparison is the peak energy per cycle, $\hat{E}_{out}^{max}$. The required energy input and the electro-mechanical conversion efficiency for dynamic operation were also calculated. Numerical values for the dynamic output energy, and output energy density per unit volume, mass, and cost were computed and comparatively presented. It was found that the dynamic energy values are, on average, 4 times lower than the static values. This is simply explained by the fact that dynamic operation needs to take place about a bias position, such that the actual dynamic amplitude is roughly half the static full travel.

The present study offers useful static and dynamic performance data that can be directly incorporated in the design of mechanical and hydraulic actuation devices utilizing off-the-shelf solid-state induced-strain actuators. The comprehensive analysis presented in the study can be readily applied to other solid-state induced-strain actuators as well as to similar products. It can also lead to industry standards that will greatly facilitate the development, use, and marketing of this novel class of actuators.

ACKNOWLEDGEMENTS

The authors gratefully acknowledge the support of the U.S. Army Research Office–University Research Initiative Program, Grant No. DAAL03-92-0181, Dr. Gary Anderson, Program Manager and of the National Science Foundation through the NSF-EPSCoR Cooperative Agreement No. EPS 09630167. The authors would also like to thank all the contact persons in the companies participating in our induced-strain actuator survey, and especially: Candace Borque from Polytec PI Inc.; Gordon Cook from EDO Corporation, Electro-Acoustic Division; Mel Goodfriend from ETREMA Products, Inc.; Andy Ritter from AVX Corporation, Research Laboratory; and Mike Konno from Tokin America, Inc., who gracefully gave their help, guidance and constructive intellectual interaction in clarifying some of the more subtle points encountered during the survey.

REFERENCES

Anon., 1988, "IEEE Standard on Piezoelectricity," ANSI/IEEE Std 176-1987, Institute of Electrical and Electronics Engineers, Inc., New York.

AVX Corporation, 1995, Product Catalogues and Private Communications, Myrtle Beach, SC 29577.

Burleigh Instruments, Inc., 1995, Product Catalogues and Private Communications, Burleigh Park, Fishers, NY 14453.

EDO Corporation, 1996, Product Catalogues and Private Communications, 2645 South 300 West, Salt Lake City, Utah 84115.

ETREMA Products, Inc., 1997, Product Catalogues and Private Communication, 2500 North Loop Drive, Ames, Iowa 50010.

Giurgiutiu, V. and Rogers, C.A., 1997a, "Large-Amplitude Rotary Induced-Strain (LARIS) Actuator," *Journal of Intelligent Material Systems and Structures*, Technomic Pub. Co., Inc., Jan. 1997, pp. 41–50.

Giurgiutiu, V. and Rogers, C.A., 1997b, "Power and Energy Capabilities of Commercially-Available Induced-Strain Actuators under Full-Stroke Dynamic Conditions," *Journal of Intelligent Material Systems and Structures*, Technomic Pub. Co., Inc., Vol. 7, No. 6, Nov. 1996, pp. 656–667.

Giurgiutiu, V., Chaudhry, Z., Rogers, C.A., 1994. "The Analysis of Power Delivery Capability of Induced-Strain Actuators for Dymamic Applications," June 5–8, 1994, Colonial Williamsburg, VA, Technomic Pub. Co., Inc., pp. 565–576.

Giurgiutiu, V., Rogers, C.A. and Chaudhry, Z., 1996, "Energy-Based Comparison of Solid-State Induce-Strain Actuators," *Journal of Intelligent Material Systems and Structures*, Vol. 7, No. 1, pp. 4–14.

Kinetic Ceramics, Inc., 1995, Product Catalogues and Private Communications, 26242 Industrial Blvd., Hayward, CA 94545.

Morgan Matroc, 1995, Electroceramics Division, Product Catalogues and Private Communications, 232 Forbes RD., Bedford, Ohio 44146.

Polytec PI, Inc., 1995, Product Catalogues and Private Communications, 3001 Redhill Ave., Bldg. 5-102, Costa Mesa, CA 92626.

Tokin America, Inc., 1995, Product Catalogues and Private Communications, 155 Nicholson Ln., San Jose, CA 95134.